



FUNCTIONAL INTEGRATION FOR ENROLMENT CONSTRAINS EVOLUTIONARY VARIATION OF PHACOPID TRILOBITES DESPITE DEVELOPMENTAL MODULARITY

by MORGANE OUDOT¹ , PASCAL NEIGE¹, RÉMI LAFFONT¹,
NICOLAS NAVARRO^{1,2} , AHMED YACINE KHALDI³ and CATHERINE CRÔNIER^{1,4,*} 

¹Biogéosciences, UMR CNRS 6282, Université Bourgogne Franche-Comté, 6 boulevard Gabriel, 21000 Dijon, France; morgane.oudot@u-bourgogne.fr, pascal.neige@u-bourgogne.fr, remi.laffont@u-bourgogne.fr

²EPHE, PSL University, 21000 Dijon, France

³Laboratoire de Paléontologie Stratigraphique et Paléo-Environnements, Université d'Oran, boîte postale 1524, El-M'naouer, 31000 Oran, Algérie;

⁴Université de Lille, CNRS, UMR 8198–Evo-Eco-Paléo, F-59000 Lille, France; catherine.cronier@univ-lille.fr

*Corresponding author

Typescript received 18 April 2018; accepted in revised form 17 January 2019

Abstract: Modularity and integration are variational properties expressed at various levels of the biological hierarchy. Mismatches among these levels, for example developmental modules that are integrated in a functional unit, could be informative of how evolutionary processes and trade-offs have shaped organismal morphologies as well as clade diversification. In the present study, we explored the full, integrated and modular spaces of two developmental modules in phacopid trilobites, the cephalon and the pygidium, and highlight some differences among them. Such contrasts reveal firstly that evolutionary processes operating in the modular spaces are stronger in the cephalon, probably due to a complex regime of selection related to the numerous functions ensured by this module. Secondly, we demonstrate that the same pattern of covariation is shared among species, which also differentiate along this common functional integration. This common

pattern might be the result of stabilizing selection acting on the enrolment and implying a coordinate variation between the cephalon and the pygidium in a certain direction of the morphospace. Finally, we noticed that *Austerops legrandi* differs slightly from other species in that its integration is partly restructured in the way the two modules interact. Such a divergence can result from the involvement of the cephalon in several vital functions that may have constrained the response of the features involved in enrolment and reorganized the covariation of the pygidium with the cephalon. Therefore, it is possible that important evolutionary trade-offs between enrolment and other functions on the cephalon might have partly shaped the diversification of trilobites.

Key words: functional integration, enrolment, developmental modularity, Phacopidae, trilobite.

COMPLEX organisms are made of recognizable anatomical parts, seemingly independent from each other (i.e. modular) but nonetheless coordinated throughout the whole organism (i.e. integrated) to ensure its functionality (Klingenberg 2008, 2014; Hallgrímsson *et al.* 2009). Thus, integration influences the direction of evolution while modularity affects the evolvability of complex systems by limiting the effect of trait variation to sets of functionally or developmentally related traits (Hallgrímsson *et al.* 2009; Clune *et al.* 2013). The explicit reference to internal factors when studying morphological variability has been incidental (Wagner & Altenberg 1996) or rare except in a few articles (Eble 2005; Gerber *et al.* 2007, 2008; Gerber & Hopkins 2011; Gerber 2014). As the anatomical parts

are semi-independent evolutionary units, analysing the differential filling of morphospace by clades (Roy & Foote 1997; Jablonski 2000) with an explicit reference to these specific variational properties has the potential to leverage our understanding of macroevolutionary patterns and of the role of modularity as a driver of phenotypic evolution (Gerber & Hopkins 2011). The variational properties that are modularity and integration are expressed at various levels of the biological hierarchy (Klingenberg 2014). Mismatches among these levels, for example developmental modules that are integrated in a functional unit, could be informative of how evolutionary processes have shaped organismal morphologies (Breuker *et al.* 2006) and allow us to understand the role of evolutionary trade-offs in

shaping clade diversification. Directional selection acting on the functional unit will involve a joint co-divergence of the independent developmental modules composing the functional unit and, over time, lineages will display strong covariation between modules within lineages as well as diverse patterns of covariation among lineages. By contrast, selection acting on one or other of the developmental modules will involve correlated responses in the other modules resulting in rather parallel evolutionary trajectories of lineages when this covariation is strong but fairly independent lineage trajectories when is not.

Phacopid trilobites constitute one of the most diversified trilobite orders living from the Early Ordovician to the Devonian–Carboniferous boundary (Crônier *et al.* 2011) as well as an emblematic example of the punctuated equilibrium (Eldredge & Gould 1972) and developmental heterochrony (Gould 1977, 1998; Alberch *et al.* 1979; McNamara 1986; Crônier & Courville 2003). Their phylogeny (Fig. 1) is rather well-known (McKellar & Chatterton 2009) even though some relationships remain a subject of debate (Oudot *et al.* 2019a). Like many current arthropods, phacopid trilobites were capable of enrolment, that is ‘volvation’ (Haug & Haug 2014; Balleiro & Grebennikov 2016). Authors have considered this behaviour to be a defence strategy against predatory pressures (Campbell 1977) or against stressful environmental perturbations such as turbidity (Speyer 1988) obtained by protecting the vulnerable ventral part. This enrolment ability is largely present within trilobites, involving different anatomical devices (see Clarkson & Henry 1973; Bruton & Haas 1997; Esteve *et al.* 2011). The thoracic

segment anatomy has frequently been used to understand the different enrolment types through the whole trilobite clade (Henry & Clarkson 1974; Esteve *et al.* 2018). Some also explored the contact zone between the different anatomical parts of the exoskeleton (Lerosey-Aubril & Angiolini 2009). Following on from this idea, our study focuses on two tagmata which are in contact when complete enrolment is achieved: the cephalon and the pygidium. However, we choose to investigate their dorsal shape as well as their covariation.

The cephalon is composed of a set of fused segments in the anteriormost part of the body, while the caudal part of the trilobite body is also formed by fused trunk exoskeletal segments, called the pygidium (Hughes 2003). In numerous trilobite taxa, and especially in phacopids, the integrity of enrolment is reinforced by the presence of special devices, i.e. a vincular furrow on the cephalic doublure (Fig. 1) into which the posterior margin of the pygidium fits with a perfect edge-to-edge fit (Whittington *et al.* 1997). Thus, these coaptative structures show a mechanical adjustment of two distinct parts (i.e. two tagmata) and ensure a perfect and passive protection of the ventral side during enrolment. To complete this mechanical adjustment, the thoracic segments are lodged in the extensions of the cephalic doublure becoming crenulated, divided into vincular notches posterolaterally. These coaptative structures are completed by panderian protuberances that control the pleural fitting at the end of the enrolment (Hupé 1953), and by a system of well-developed articular facets. Bruton & Haas (1997) have thoroughly studied these coaptative structures in phacopids to

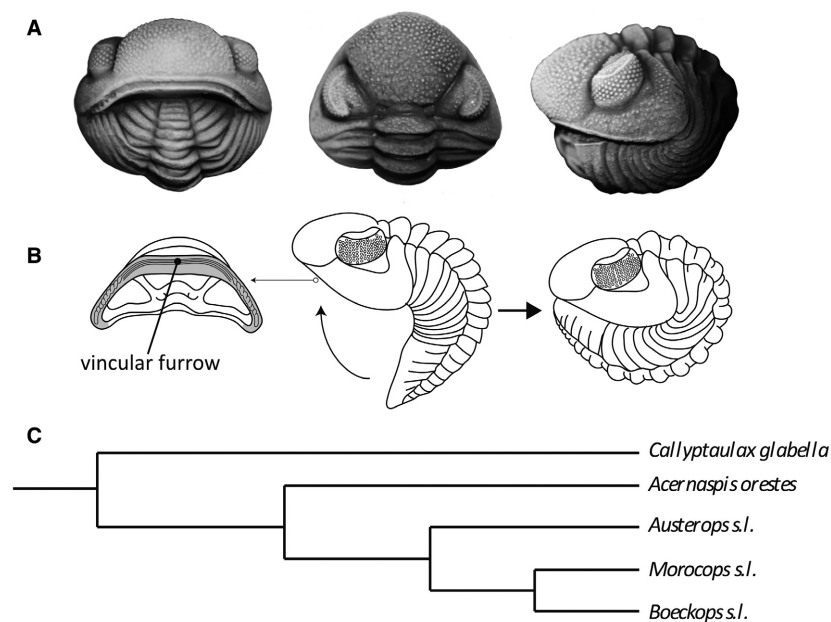


FIG. 1. A, *Morocops granulops* (after Khaldi *et al.* 2016) in frontal, dorsal and lateral views. B, illustration of the phacopid enrolment and coaptative structures associated in ventral view of the cephalon and lateral view of the entire exoskeleton. C, summary of phacopid phylogeny (after McKellar & Chatterton 2009 and Oudot *et al.* 2019a).

demonstrate diverse protective adaptations and different strategies of enrolment in closely related taxa of this family. In our study, all studied phacopids share the same coaptative devices. Therefore, phacopids appear to be a good model for exploring the constraints produced by functional relationships on divergences of developmental modules since several enrolling strategies have been explored over the 130 myr of their existence in the Palaeozoic Era.

The cephalon together with the trunk tagma is considered to be the ancestral condition of tagmosis in trilobites, whereas the pygidium is a functionally distinct tagma derived from posterior segments that evolved secondarily (Hughes *et al.* 2006). Besides its involvement in enrolment with the pygidium, the cephalon is thought to support feeding, digestion and cognition functions, and be subject to significant ontogenetic changes in relation to changes in feeding habits (Fortey & Owens 1999; Hughes 2003). Hence, the cephalon and the pygidium appear functionally related via enrolment but also partly distinct (as the cephalon is involved in specific functions) and they are probably developmentally rather well separated. Accordingly, therefore, the cephalon shape might be expected to be under a strong and diverse selection regime, which might imply some trade-offs between its various functions and the enrolment, whereas the divergence of the pygidium shape might be neutral or under a less complex selection regime mainly related to its involvement in enrolment. In such a case of neutral divergence, among-species variation in the pygidium might be unstructured alongside covariation in the cephalon. On the contrary, a large modular variation among species affecting the cephalon is to be expected if the trade-offs between the various functions are not too strong. If some directional selection acts on the enrolment itself, we might expect to observe diverse covariation among species, whereas a stabilizing selection will involve a unique and strong pattern of covariation between the two tagmata.

Contrasting the pattern of species divergence in either the variation related to the enrolment or the variation independent of such enrolment appears to be a good rationale for evaluating current assumptions. Using geometric morphometrics, we described the shape of the two tagmata from five closely related species with well preserved and spatiotemporally circumscribed samples, and compute four different but complementary morphospaces: the full, the integrated (i.e. covarying shapes) and the modular spaces, following the approach of Mitteroecker & Bookstein (2008). Modular spaces are representative of the independent variation of the two structures, whereas variation within the covariation space refers to the functional integration of these structures. Furthermore, we assess how this covariation may have

constrained species divergences on these two developmental modules. Finally, the observation of variation above the species-level (i.e. shape disparity) within each of the four morphospaces will inform us on the potential of these spaces to embed informative evolutionary dynamics at a broader scale.

MATERIAL AND METHOD

Phacopid sampling

The studied material comes from two newly described sections (Khaldi *et al.* 2016) designated ‘Marhouma’ and ‘Erg el Djemel’, and located in the Saoura Valley, in the eastern part of the Ougarta Basin, Algerian Sahara (Fig. 2). Both are of upper Emsian age (Khaldi *et al.* 2016).

Over the last decade, numerous new phacopid faunas have been described from North Africa (Chatterton *et al.* 2006; Klug *et al.* 2009; McKellar & Chatterton 2009; Khaldi *et al.* 2016). The Algerian material, collected mainly by Y. Khaldi (Oran University), comprises 166 specimens of phacopids, collected from five levels in the Erg el Djemel section and one level in the Marhouma section, all upper Emsian in age. Taxonomic identification has been made by three of the authors (CC, MO, AYK).

After checking for preservation issues and species representativeness, 134 cephalons and 81 pygidiums (actually associated with a cephalon) were conserved: all 134 cephalons are used in the PCA analysis while the set of 81 associated cephalons and pygidium are used in covariation

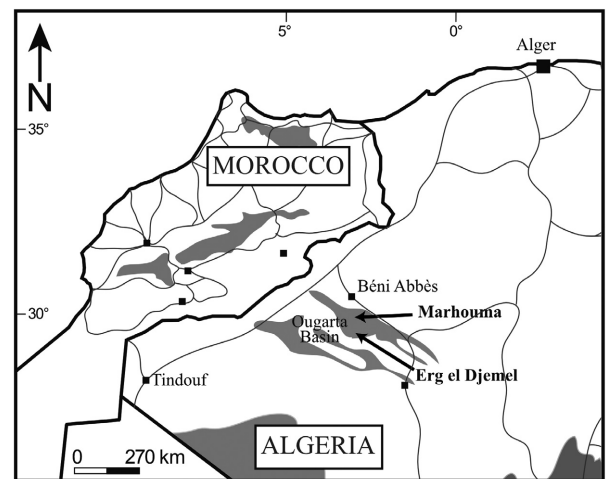


FIG. 2. Geographical location of the studied phacopid trilobites from two newly described sections: ‘Erg el Djemel’ and ‘Marhouma’ sections in the Saoura Valley, Algeria. Relief is shown in grey.

TABLE 1. Sample size of each species studied.

Sample sizes per species						
	<i>A. legrandi</i>	<i>A. menchikoffi</i>	<i>A. speculator</i>	<i>M. chattertoni</i>	<i>M. granulops</i>	Total
Cephalon	53	29	12	35	5	134
Pygidium	29	20	5	23	4	81

and modular analyses. These specimens (see Table 1 for sample sizes by species) are representatives of *Austerops legrandi* Khaldi *et al.*, 2016, *A. menchikoffi* (Le Maître, 1952) (= *Phacops smoothops* Chatterton *et al.*, 2006; see Khaldi *et al.* 2016), *A. speculator* (Alberti, 1969), *Morocops chattertoni* (Khaldi *et al.*, 2016) (*Morocops* Basse, 2006 = *Barrandeops* McKellar & Chatterton, 2009; see van Viersen *et al.* 2017), and *M. granulops* (Chatterton *et al.*, 2006). The studied specimens come from similar assemblages to minimize variation in external factors (i.e. environmental differences) and to focus rather on the internal factors, (i.e. the functional and developmental differences), and also to understand such diversity. Additionally, all studied phacopid individuals belong to holaspide instars typically composed of 11 articulated thoracic segments involved in the enrolment as well as the cephalon and pygidium (Crônier *et al.* 2011). The holaspide period begins when the number of thoracic segments specific to the species is acquired, with the functional completion of the final articulation between the last thoracic segment and the posterior shield made of merged segments (Hughes *et al.* 2006).

Imaging, digitizing and geometric morphometrics

All specimens were photographed using either a Canon PowerShot S2 IS camera (5.0 megapixels) on a binocular Zeiss Stemi SV11-Apo (by CC at the University of Lille), or a Pentax K3 camera with the HD PENTAX-DA 35 mm F2.8 Macro Limited lenses (MO at the University of Burgundy). The cephalon and the pygidium of 35 specimens were photographed twice; removing and replacing the specimen under the camera between the two shots to assess the measurement error.

As most of the specimens were partly preserved, only the right-side of each structure was considered (using the mirror function when only the left-side of the structure was preserved). To describe the morphology of these organisms, a set of 19 2D-landmarks on the cephalon and 8 2D-landmarks on the pygidium were digitized using tpsDig (Rohlf 2004, 2015) to summarize the general cephalic shape (Fig. 3); of these five and three are on the symmetry axis of the cephalon and pygidium respectively. For the 35 specimens photographed twice, each structure

was also digitized twice. To avoid problems related to treating only half of a bilateral structure (Cardini 2016), the left side of cephalon and pygidium were reconstructed by symmetrizing the right-side landmarks using the unpaired landmarks lying on the symmetry line.

Nevertheless, some specimens were more damaged than others so some landmarks were coded as ‘missing landmarks’ on some individuals; these were estimated to reconstruct a complete database of landmarks for each specimen (Gunz *et al.* 2009; Couette & White 2010). As a maximum of three landmarks are missing per side of each structure, estimating their coordinates corresponds to an increase of 1.42% in the whole data set of landmarks coordinates, which is considered here to be few enough to avoid a negative impact on the analysis. We chose to estimate missing landmarks coordinates (and preserve the initial number of specimens) using a TPS interpolation (see Gunz *et al.* 2009), through the `estimate.missing()` function from the geomorph R (v. 3.4.4) package (v. 3.0.6; Adams & Otárola-Castillo 2013).

Finally, these reconstructed configurations were subjected to two separate partial generalized Procrustes analyses (Dryden & Mardia 1998) to remove effects of size, location and orientation, and keeping only the symmetric variation of shape. Shapes were projected in the space that is tangent to the mean shape of either the cephalon or the pygidium. The resulting tangent coordinates correspond to the symmetric shapes of those anatomical structures and are used in our analyses. Cephalon and pygidium sizes were computed as their centroid size, that is the square root of the sum of squared distances from each landmark to their centroid (Dryden & Mardia 1998). This was performed by using the `bilat.symmetry()` function from geomorph (see Oudot *et al.* (2019b) for the resulting landmark coordinates).

The imaging and digitizing protocol described above allows for the assessment of two components of measurement error: the projection error (i.e. the setting of a specimen under the camera) and the digitization error. This assessment was done through Procrustes ANOVA (Klingenberg & McIntyre 1998) performed using the `procD.lm` function of Geomorph. It appears that both imaging and digitizing errors were negligible compared to individual variation.

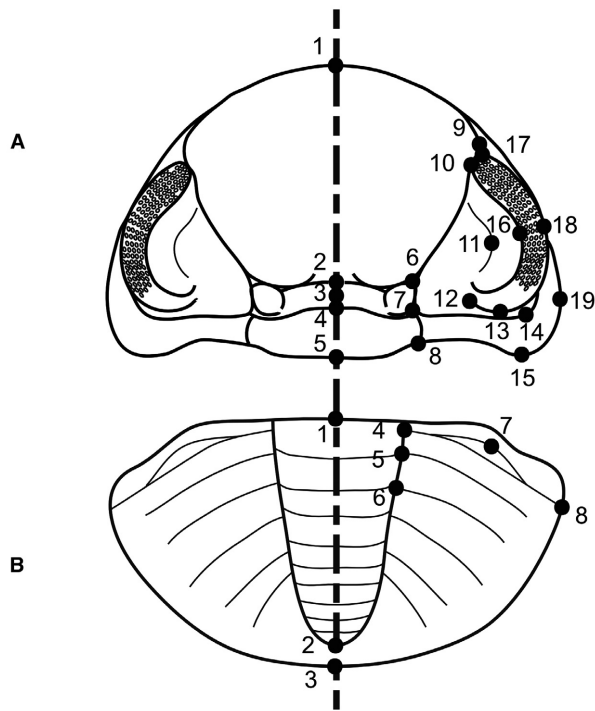


FIG. 3. Landmarks selected for morphometric analyses. Landmarks are captured in dorsal view and defined as follows: A, cephalon: 1, anteriormost midpoint of frontal lobe; 2, posterior midpoint of frontal lobe; 3, middle midpoint of preoccipital lobe; 4, posterior midpoint of preoccipital lobe; 5, posterior midpoint of occipital ring; 6, flexure point at antero-lateral angle of preoccipital lobe; 7, flexure point at postero-lateral angle of preoccipital lobe; 8, flexure point between posterior margin of occipital lobe and posterior border; 9, most lateral point on frontal lobe; 10, point of anterior innermost edge of eye; 11, middle point at maximum curvature of palpebral furrow; 12, point of posterior innermost edge of eye; 13, posteriormost maximum curvature of eye; 14, posteriormost maximum curvature of the posterior border furrow; 15, most posterior point on posterior border; 16, middle point at maximum curvature of dorsal edge of eye; 17, anteriormost maximum curvature of eye; 18, middle point at maximum curvature of ventral edge of eye; 19, most lateral point on lateral border; B, pygidium: 1, anteriormost midpoint of pygidial axis; 2, posterior midpoint of pygidial axis; 3, posteriormost midpoint of posterior border; 4, intersection of first interpleural furrow with dorsal furrow; 5, intersection of second interpleural furrow with dorsal furrow; 6, intersection of third interpleural furrow with dorsal furrow; 7, anterior point of maximum curvature of articulating half rib; 8, lateral extremity of articulating facet.

Decomposing the morphospace: full, integrated and modular spaces

Major patterns of shape variation were examined within a reduced shape space obtained from principal component analysis (PCA) of the variance–covariance matrix of

the tangent coordinates, computed using the `plot Tangentspace()` function of `geomorph`. This full shape space could be divided into three subspaces: an integrated shape space and two modular spaces, one for each structure from which the covariation is studied (Mitteroecker & Bookstein 2008). Mitteroecker & Bookstein (2007) defined a model of common and local developmental factors, each of them affecting phenotypic variables differently. Local factors influence the morphological variation of only one module, whereas common factors affect traits of different modules. Thus, modules are constructed as anatomical parts that are separately influenced by dissociated local factors while they may also be integrated through some common factors. According to this model, the integrated space is ordinated by scores along common factors (developmental factors affecting traits of different modules) whereas the modular spaces are ordinated by scores along local factors (that influence the morphological variation of one module only).

In the first instance, to check if a common integrated space is computable, we performed separate partial least squares (PLS) analyses for each species whose sample size is greater than 20 individuals (i.e. *A. legrandi*, *A. menchikoffi* and *M. granulops*) and computed pairwise angular comparisons between these species. These angles were statistically tested against random null distribution of angles computed from multidimensional pairs of vectors (Klingenberg *et al.* 2003). As there were no differences among the first PLS vector of each species, the common integrated space was assessed using two block PLS analysis (2B-PLS, Rohlf & Corti 2000) on the cross-covariance matrix between cephalon and pygidium tangent coordinates computed by using the `two.b.pls()` function of `geomorph`. As species differences may confound the covariation pattern between modules, the variance–covariance matrix was pooled by species to avoid this potential effect on the computation of shape covariances. Nevertheless, scores of individuals were computed on unpooled data (so taking into account the species mean). The significance of each PLS pair was obtained following the approach of Mitteroecker & Bookstein (2008), based on 1000 permutations of observations from residual data matrices. Only the first significant PLS pairs were kept to describe the integrated space.

To assess whether species share the same pattern of integration, we used the previous separate PLS vectors (on both modules and stacked vectors) from each species and performed pairwise angular comparisons with the common PLS vector of integration. Furthermore, to test if morphological differences can be linked with the common pattern of covariation, we computed a pairwise angular comparison between species contrasts (i.e. pairwise difference of mean shape between species) and the

common PLS vector of integration (on both modules and stacked vectors). These angles were tested against random null distribution of angles computed from multidimensional pairs of vectors (Klingenberg *et al.* 2003).

Modular spaces of the cephalon and the pygidium were then computed as orthogonal to the whole covariation pattern (i.e. first significant PLS pairs), following the approach of Mitteroecker & Bookstein (2008). The shapes of each tagma were projected orthogonally to the normalized first pair of singular vectors obtained from the 2B-PLS, resulting in a morphospace with all the shape variations but those related to common factors (Mitteroecker & Bookstein 2008). In other words, the full shape space was decomposed according to an integrated space relating to the within-species morphological covariation and two modular spaces orthogonal to that covariation. R codes computing the orthogonal spaces are available in Oudot *et al.* (2019b).

Assessing species differences in the four spaces

Species differences were evaluated using Procrustes ANOVAS, which deal only with the amount of variation. When significant, pairwise Hotelling T^2 tests (using Hotelling, v. 1.0-4 package, Campbell & Curran 2009) were performed to evaluate pairwise species differences, using a BH adjustment to control the false discovery rate (Benjamini & Hochberg 1995). The integration and modular spaces were computed on the species-pooled covariance matrix so that species differences do not impeded the covariance between the two developmental modules. To test for species differences in that space, we therefore reprojected the mean shapes of species and added them to the scores of individuals before comparison and visualization.

RESULTS

Shape variation

For cephalon, morphological relationships among individuals can be visualized through the morphological space (Fig. 4), defined by the first three principal component axes. The first PC explained 47.24% of the observed variation among individuals, the second, 14.00%, and the third, 7.5%. The morphological changes associated to each PC are depicted through thin plate spline deformation grids (Fig. 4). The PC1 axis shows that the main shape change in these species contrasts more or less large cephalon (with or without stretched genal angles) while the PC2 axis shows more or less parabolic cephalic outline and the PC3 axis depicts more or less inflated glabella.

Species are well differentiated in morphospace mainly along the first axis where *Austerops legrandi* is very well individualized, while *A. menchikoffi* and *A. speculator* overlap. *Morocops granulops* appears rather differentiated, even if *M. chattertoni* seems to overlap a little. The Procrustes ANOVA (keeping 80% of the explained variance) confirmed this visual inspection of the scatterplots as significant species effect was observed ($F_{df=4} = 14.03$, $p < 0.001$). Pairwise Hotelling T^2 tests (Table 2) revealed that *Austerops legrandi* is significantly different from other species. Actually, and despite some overlaps, all species are significantly different from one another.

For pygidia, morphological relationships among studied individuals can be displayed in the morphological space (Fig. 5) defined by the first three principal component axes. The first PC explained 46.24% of the observed variation among individuals, the second, 20.63%, and the third, 16.08%. The morphological changes associated with each PC are depicted through thin plate spline deformation grids (Fig. 5). The PC1 axis shows that the main shape change in these species contrasts a more or less large pygidium (with a more or less parabolic outline) while the PC2 axis shows a displacement of the maximal bulging of the pygidium along the pygidial axis (with an elongation of the pygidial end), and the PC3 axis depicts a more or less inflated pygidial axis.

Unlike cephalon, species seem to overlap a lot more when considering pygidia. Nonetheless, Procrustes ANOVA (keeping 80% of the explained variance) revealed a species effect ($F_{df=4} = 6.24$, $p < 0.001$) and the pairwise Hotelling test demonstrates that all the species are significantly different, except *A. speculator* and *M. chattertoni* which are not (Table 3).

Integrated space

The 2B-PLS was performed on the species-pooled cross-covariance matrix of tangent coordinates between the pygidium and the cephalon and then, graphically visualized by reprojecting species mean onto PLS vectors of the pooled data (Fig. 6). The permutation test of Mitteroecker & Bookstein (2008) revealed that only the first PLS pair (which accounts for 71.82% of the total squared cross covariance) is significant. Other PLS pairs are thus not shown in the following results.

The first PLS axis related to the cephalon involves an increasingly stockier glabella that is less angular in its anterior part and narrower in its posterior part, with a stretching of the genal angles. The first PLS axis related to the pygidium involves an elongation (sag.) of the pygidial axis concurrent with the evolution of the global shape from an open circular arc to a closed one.

In this plot, species overlap a lot and more or less follow a line representing the covariation link between the

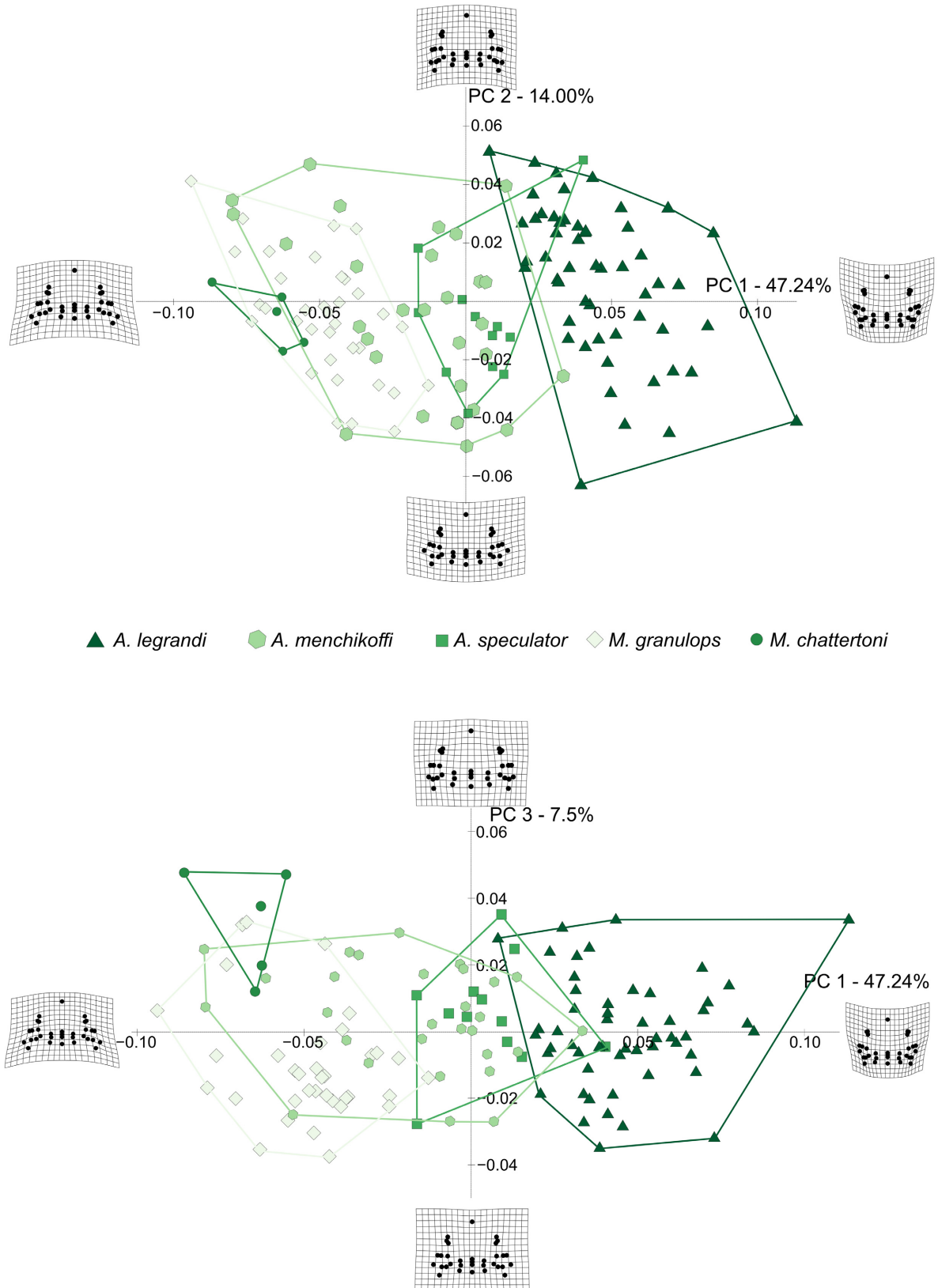


FIG. 4. Principal components analysis performed on the database of 134 cephalons, (top) PC1–PC2 plane and (bottom) PC1–PC3 plane. Thin plate splines depict the extremes of cephalon shape on each axis edge. Colour online.

TABLE 2. Results of pairwise Hotelling test on the cephalon, within the full shape space (top) and the modular shape space (bottom).

Pairwise Hotelling on full morphospace					
	<i>A. legrandi</i>	<i>A. menchikoffi</i>	<i>A. speculator</i>	<i>M. chattertoni</i>	<i>M. granulops</i>
<i>A. legrandi</i>	/	343.10	157.38	284.83	1094.11
<i>A. menchikoffi</i>	0.000	/	21.42	47.95	165.24
<i>A. speculator</i>	0.000	0.014	/	121.74	179.65
<i>M. chattertoni</i>	0.000	0.001	0.001	/	46.81
<i>M. granulops</i>	0.000	0.000	0.000	0.000	/
Pairwise Hotelling on modular morphospace					
	<i>A. legrandi</i>	<i>A. menchikoffi</i>	<i>A. speculator</i>	<i>M. chattertoni</i>	<i>M. granulops</i>
<i>A. legrandi</i>	/	149.61	50.00	176.23	580.42
<i>A. menchikoffi</i>	0.000	/	6.56	23.87	67.65
<i>A. speculator</i>	0.000	0.131	/	68.63	89.26
<i>M. chattertoni</i>	0.000	0.004	0.004	/	16.15
<i>M. granulops</i>	0.000	0.000	0.000	0.007	/

Significant p-values are shown in **bold**.

two anatomical structures. Nevertheless, the Procrustes ANOVA (performed on reprojected data) shows a significant difference in the covariation link between the cephalon and the pygidium among species ($F_{df=4} = 7.10$, $p < 0.001$). Pairwise Hotelling tests (Table 4) reveal that *A. legrandi* is significantly different from other species, except *A. speculator*. Furthermore, *A. menchikoffi* is significantly different from other species but not from *M. granulops*. *M. granulops* and *M. chattertoni* also appear as non-different, while other species remain different from each other.

All angles between the first pair of PLS (both common and species vectors) are significantly different from random angles (Table 5) meaning that all these vectors share a common direction of integration. Nevertheless, *A. legrandi* diverges slightly from the common PLS vector compared to other species. If we now consider modules separately, the pygidium exhibits higher angular values than the cephalon (see Oudot *et al.* 2019b, table S1). Moreover, the angular comparison between species contrasts and the main vector integration (Table 6) shows that these angles differ from random, aside from the angular comparison between the integration vector and the contrast opposing *M. granulops* and *M. chattertoni*.

Modular spaces

As an orthogonal space of the integrated morphospace, the modular spaces are devoid of dimensions of integrated shape variation (Fig. 6). Thus, in such an orthogonal space each anatomical structure is treated individually

(Figs 7, 8) and shape differences depicted by these spaces reflect differences due to local factors, that is modular shape variation. For cephalon, the first three PCs of the modular space (Fig. 7) account for almost 67% of the modular variance. The PC1 axis mainly contrasts more or less rounded cephalon while the PC2 axis shows the transition from a much broader glabella to a much narrower one and PC3 distinguishes a more or less inflated cephalon. For pygidia (Fig. 8), the first three PCs of the modular space account for almost 82% of the modular variance. PC1 sustains the transition from a straight pygidial anterior margin to a much more rounded one and PC2 contrasts more or less splayed pygidial segments and a pygidial axis short to much longer while PC3 distinguishes a swollen pygidial axis to a much flat one.

The five species occupy quite distinct regions in the modular space of the cephalon. In fact, computing convex hulls around each species mean shows that each species is rather well defined. *Austerops legrandi* is the most different and is very well isolated from other species; the others are much closer together but still remain different from one another. By contrast, in the modular space of the pygidium the five species are not that well defined, and the species strongly overlap each other. Thus, even though species remain distinguishable from one another, they are clearly much better defined in the modular space of the cephalon.

Procrustes ANOVA (keeping the first three axes) points to similar conclusions, as significant species effect was observed both on the modular cephalon and pygidium ($F_{df=4} = 12.08$, $p < 0.001$; $F_{df=4} = 4.04$, $p < 0.001$ respectively). For the cephalon, pairwise comparisons revealed that species are clearly different from one

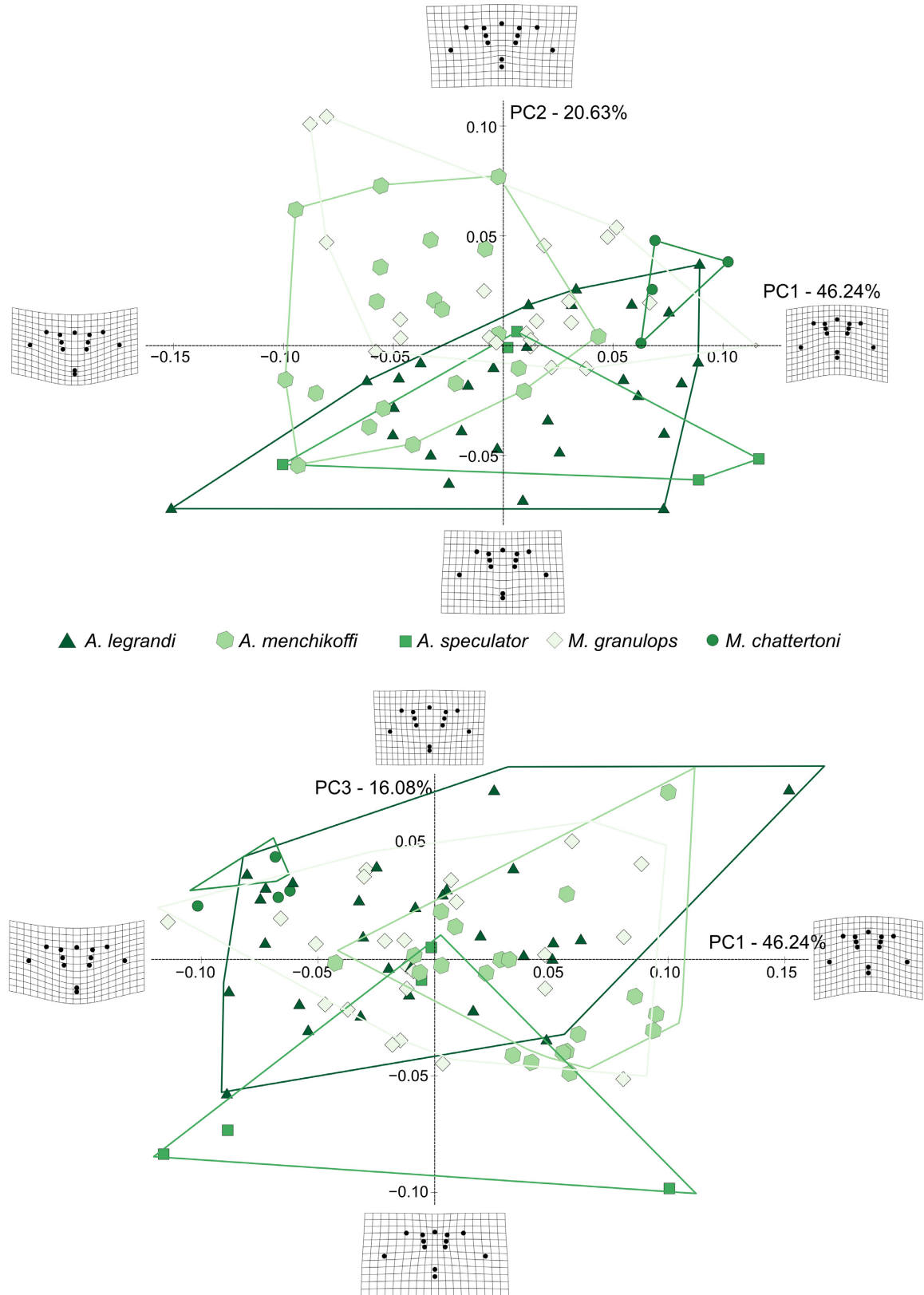


FIG. 5. Principal components analysis performed on the database of 81 pygidia, (top) PC1–PC2 plane and (bottom) PC1–PC3 plane. Thin plate splines depict the extremes of pygidium shape on each axis edge. Colour online.

TABLE 3. Results of pairwise Hotelling test on the pygidium, within the full shape space (top) and the modular shape space (bottom).

Pairwise Hotelling on full morphospace					
	<i>A. legrandi</i>	<i>A. menchikoffi</i>	<i>A. speculator</i>	<i>M. chattertoni</i>	<i>M. granulops</i>
<i>A. legrandi</i>	/	32.48	19.24	27.23	24.07
<i>A. menchikoffi</i>	0.000	/	15.19	36.10	12.72
<i>A. speculator</i>	0.000	0.014	/	14.48	18.69
<i>M. chattertoni</i>	0.004	0.000	0.094	/	14.56
<i>M. granulops</i>	0.000	0.015	0.007	0.021	/

Pairwise Hotelling on modular morphospace					
	<i>A. legrandi</i>	<i>A. menchikoffi</i>	<i>A. speculator</i>	<i>M. chattertoni</i>	<i>M. granulops</i>
<i>A. legrandi</i>	/	20.24	12.04	14.35	12.81
<i>A. menchikoffi</i>	0.000	/	4.52	34.13	17.30
<i>A. speculator</i>	0.031	0.263	/	12.59	4.88
<i>M. chattertoni</i>	0.030	0.000	0.161	/	13.88
<i>M. granulops</i>	0.015	0.007	0.235	0.030	/

Significant p-values are shown in **bold**.

another, except for *A. menchikoffi* and *A. speculator* (Table 2). In contrast, for the pygidium (Table 3), *A. speculator* cannot be differentiated from any other species except *A. legrandi*. Moreover, statistical values from each pairwise comparison are much weaker than those obtained from comparisons of cephalon.

DISCUSSION

Cephalon and pygidium shape provides taxonomically relevant variation supportive of other diagnostic characters of species (ornamentation, number of lens files per

eye and of lenses per file, presence/absence of a subocular pad etc.) The cephalon of *Austerops legrandi* seems to have an original shape in comparison to other species. Indeed, this species has a glabella with a very wide base, which differentiates it from other representatives of *Austerops*. *Austerops speculator* and *Morocops chattertoni* are also significantly different from other species despite some overlap. On the other hand, *Austerops menchikoffi* and *Morocops granulops* do not differ from one another in overall cephalon shape. In fact, according to their morphological description (Chatterton *et al.* 2006), these two species are quite similar in overall size and shape but differ in meristic traits, *M. granulops* having coarser and

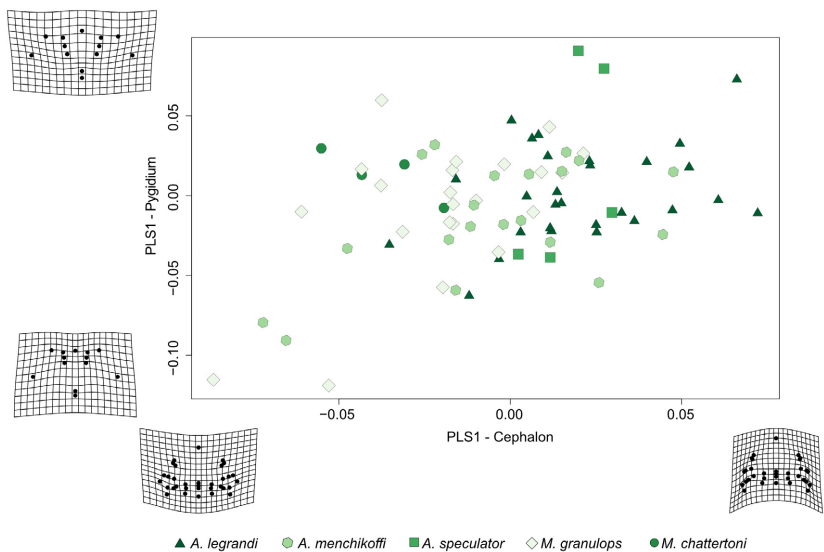


FIG. 6. Two-block partial least squares (PLS) plot performed on 81 individuals with cephalon and pygidium associated. This plot shows the first pair of PLS axes (first axis of the cephalon and first axis of the pygidium); thin plate splines depict the extremes of cephalon and pygidium shape on each axis edge. Colour online.

TABLE 4. Results of pairwise Hotelling test on the integrated space.

Pairwise Hotelling on the first pair of PLS					
	<i>A. legrandi</i>	<i>A. menchikoffi</i>	<i>A. speculator</i>	<i>M. chattertoni</i>	<i>M. granulops</i>
<i>A. legrandi</i>	/	22.49	5.04	20.43	32.05
<i>A. menchikoffi</i>	0.000	/	13.15	11.48	4.96
<i>A. speculator</i>	0.105	0.013	/	38.50	12.03
<i>M. chattertoni</i>	0.000	0.013	0.003	/	6.20
<i>M. granulops</i>	0.000	0.110	0.013	0.095	/

Significant p-values are shown in **bold**.

TABLE 5. Results of angular comparisons between the first pair of PLS of each species (sample size >20 individuals).

Angular comparison between the first pair of PLS (both common and species)				
	Common	<i>A. legrandi</i>	<i>A. menchikoffi</i>	<i>M. granulops</i>
Common	/	54.92	28.69	28.69
<i>A. legrandi</i>	$<1 \times 10^{-5}$	/	74.04	66.52
<i>A. menchikoffi</i>	$<1 \times 10^{-5}$	8e-04	/	36.24
<i>M. granulops</i>	$<1 \times 10^{-5}$	1e-04	$<1e-05$	/

TABLE 6. Results of angular comparisons between species contrasts and the vector of integration.

Angular comparison between PLS1 and contrasts		
	Angle value	p-value
PLS1 vs <i>A. legrandi</i> – <i>A. menchikoffi</i>	58.88	9.99×10^{-6}
PLS1 vs <i>A. legrandi</i> – <i>A. speculator</i>	75.26	0.014
PLS 1 vs <i>A. menchikoffi</i> – <i>A. speculator</i>	40.99	9.99×10^{-6}
PLS 1 vs <i>M. granulops</i> – <i>M. chattertoni</i>	88.60	0.817
PLS1 vs <i>Austerops</i> – <i>Morrocops</i>	63.84	2.99×10^{-5}

denser tubercles, one more file of lenses (19 in *M. granulops* vs 18 in *A. menchikoffi*), a lower number of lenses per file and a subocular pad. Although our analysis of the pygidium full morphospace leads to similar conclusions, the amount of overlap between species appears larger than for cephalon morphospace. It suggests that with the concentration of many vital functions in the cephalon (Fortey & Owens 1999; Hughes 2003), this structure accumulates a greater interspecific divergence in shape (i.e. greater disparity).

The modular spaces of the two tagmata appear to contain species-level variation as significant differences among species were observed. Nevertheless, species divergences on the pygidium are statistically weaker than on the cephalon. Therefore, it appears that the two anatomical structures bear quite different information: the

cephalon provides strong additional support for taxonomic units even after removing its covarying part, while the pygidium, once deprived of its covarying part, only weakly supports taxonomic separation.

The cephalon is composed of several anatomical/developmental modules (Hughes 2003; Gerber & Hopkins 2011) which appear here to vary to some extent among species. Indeed, the cephalon is a complex structure, which directly and indirectly supports many functions, such as feeding, digestion and cognition. It is also the locus of major morphological innovations (Hughes 2007), arguably devoted to specific functions (Gerber & Hopkins 2011), especially in the frontal area (the prelabellar and preocular areas) including, for example, the projecting trident of some Devonian trilobites (Hughes 2007). Moreover, as the cephalon is the site of ingestion and food processing, changes in cephalic morphology may be related to changes in feeding habits during growth, as larger individuals are able to feed on bigger prey (Hughes 2003).

Either way, it seems that evolutionary processes do operate in such modular spaces, even though it appears stronger with the cephalon rather than with the pygidium. Given the likelihood of a more complex selection regime on the cephalon related to its numerous functions (compared to that of the pygidium) we can expect such differential divergences in the modular spaces if the trade-offs among the cephalon features are not too strong, which appears to be the case. Disentangling the role of selection to drift in pygidium divergence is trickier given the less documented functional assumptions on this structure as well as the material we have in hand.

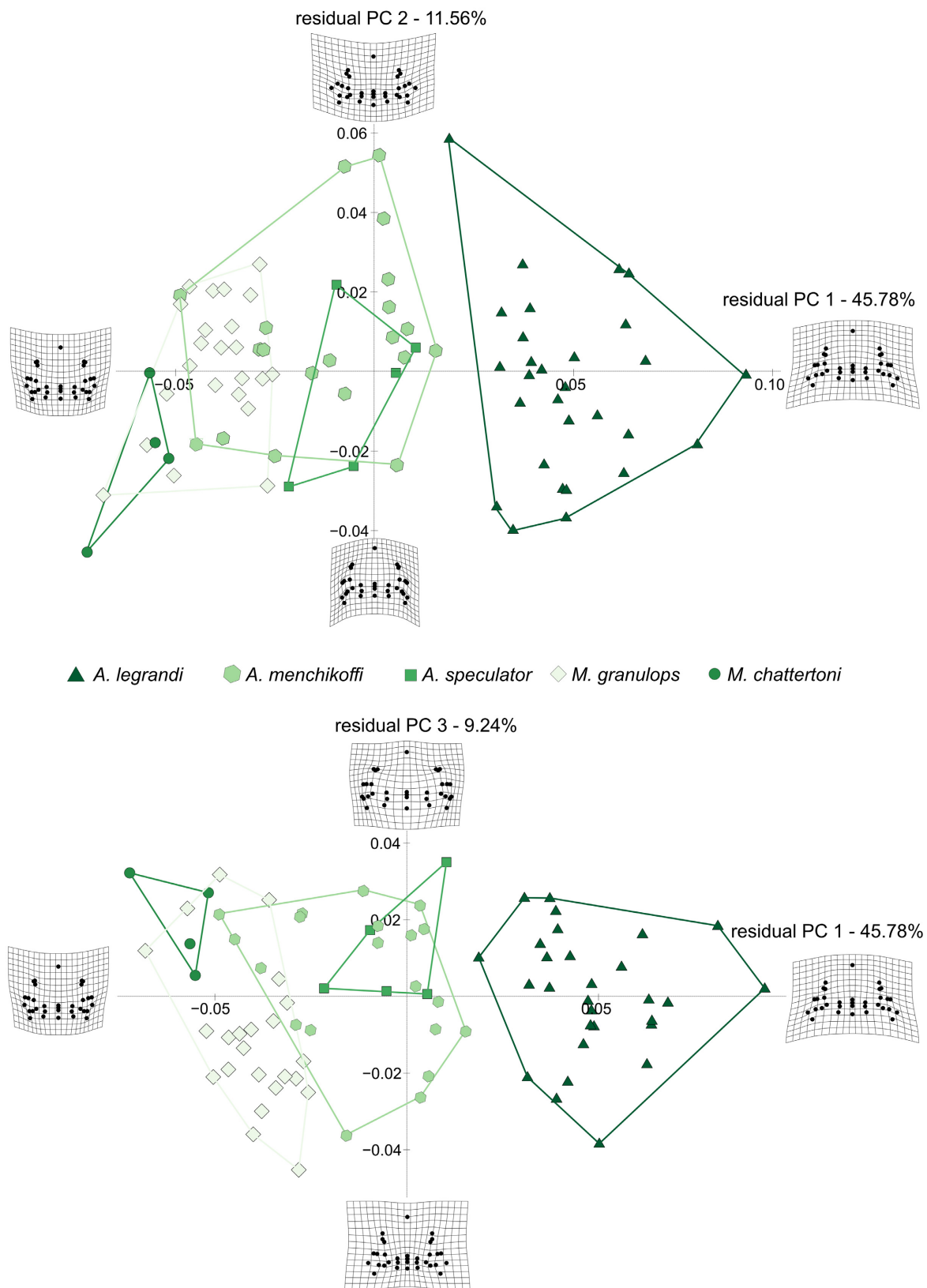


FIG. 7. Modular space of the 81 cephalons (associated with pygidia) along the PC1-PC2 plane (top) and PC1-PC3 plane (bottom), with thin plate splines depicting extremes of cephalon shape. Colour online.

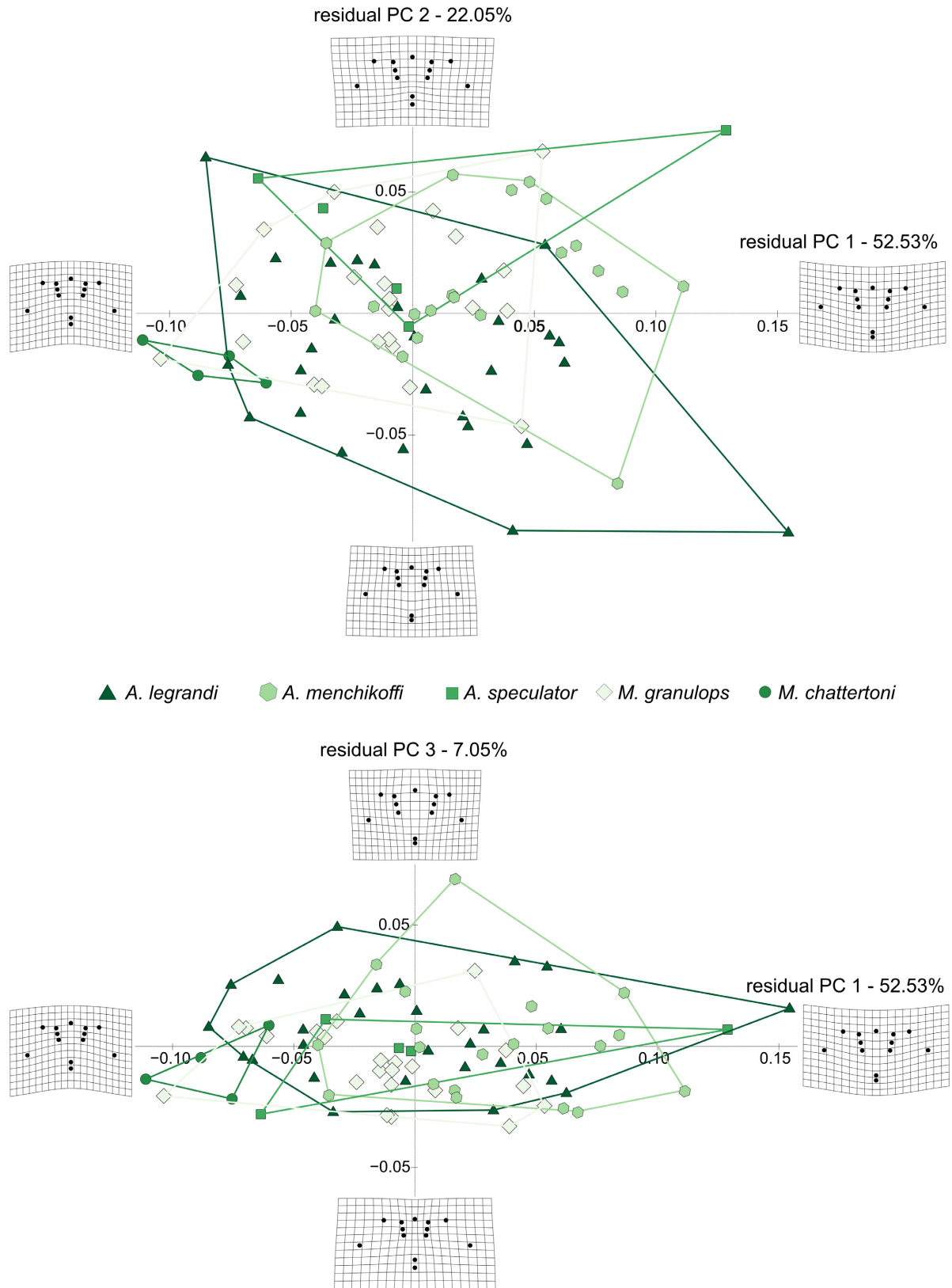


FIG. 8. Modular space of the 81 pygidia (associated with cephalae) along the PC1–PC2 plane (top) and PC1–PC3 plane (bottom), with thin plate splines depicting extremes of pygidium shape. Colour online.

In phacopid trilobites, the integrity of enrolment is reinforced by the presence of a vincular furrow on the cephalic doublure in which the posterior margin of the pygidium fits (a coaptative feature), which ensures full protection of the ventral side. Therefore, the two anatomical structures involved in volvation must spatially accommodate each other to guarantee the functional integrity of enrolment. Most of this spatial accommodation lies in the glabella becoming stockier on the cephalon while the pygidium evolves from an open circular arc to a closed one. Such phenotypic integration imposes constraints on the morphological variation, limiting the number of accessible phenotypes that are possible (Gerber 2014). At first sight, species seem to share the same integration: their main pattern of integration (i.e. PLS vector) is roughly oriented with the common one, with angles between them smaller than those between two random vectors. Given this relative common integration, strong directional selection on the coordination of the two developmental modules for enrolment seems not be operating at the level of our studied clade (for similar results, see Machado *et al.* 2018). Species overlap in the integrated space despite some significant differentiation. Indeed, comparison of species contrasts and the main axis of integration reveals that species, or even genera, differentiate along the common integration. Thus, species and even genera would globally share a same integrated pattern but still, divergence and differentiation operate along this main axis. Such a differentiation lined up with the integrated pattern suggests that evolutionary divergences are partly channelled. Thus, stabilizing selection might be acting weakly on enrolment and we can envisage that it might lead to an extreme end-result: the loss of detectable covariation at an intraspecific-level but its preservation from an interspecific point of view (Armbruster & Schwaegerle 1996; Armbruster *et al.* 2004, 2014; Klingenberg 2014). Either way, this functional integration implies the coordinated variability of functionally related parts, and so, allows for differentiation in a certain direction in the morphological space (for similar results and hypotheses, see e.g. Young 2006; Guillaume & Otto 2012; Rueffler *et al.* 2012; Armbruster *et al.* 2014).

It should be noted that integration in *Austerops legrandi* appears to be partly restructured. This reorganization affects mainly the pattern of covariation on the pygidium. Such divergence in the way the two developmental modules interact indicates that directional selection was probably acting on enrolment in this species (for similar results see e.g. Penna *et al.* 2017; Machado *et al.* 2018). The weaker response in the cephalon than in the pygidium could be related to the involvement of the cephalon in its many other functions. The possible role of directional selection within functional module (i.e. enrolment) was previously suggested by Wagner (1996), while other modules

(involved in other functions ensured by the cephalon) could be influenced by other regimes of selection. These features (i.e. nutrition, cognition functions, etc.) may have constrained the selection response of those involved in enrolment by reorganizing the way the pygidium covaries with the cephalon. Therefore, it is probable that important evolutionary trade-offs between the enrolment and the other vital functions borne by the cephalon might have been operating during the diversification of trilobites.

On the other hand, enrolment itself is a major factor that may trigger the successful evolution of trilobites, as suggested by Laibl *et al.* (2016) and Ortega-Hernández *et al.* (2013) for trilobites from the Cambrian, or even through the entire Paleozoic (Clarkson & Henry 1973; Henry & Clarkson 1974; Babcock & Speyer 1987; Esteve *et al.* 2011) even if trilobites did not achieve full enrolment in Cambrian times because of the poor development of interlocking devices (Esteve *et al.* 2011). Complete enrolment is exhibited by trilobites following the development and the proliferation of coaptative devices, which appeared mainly in post-Cambrian times with the evolution of a fulcrate exoskeleton (Clarkson & Whittington 1997). These new morphological devices apparently evolved abruptly, but once established show only minor improvement and/or a gradual evolutionary improvement of the mechanical adjustment as a whole (Clarkson & Whittington 1997).

Recently, Laibl *et al.* (2016) demonstrated the presence of several enrolment styles in a Cambrian family (Paradoxididae) demonstrating encapsulated and probably non-encapsulated enrolment, and suggesting independent evolution among its representatives due to different environments or rapid changes in abiotic factors. In the same way, Esteve & Yuan (2017) compared specimens from two different lineages (odontopleurids and asaphids) and showed that although odontopleurids were very conservative (using the same enrolment style throughout their history in more or less the same niches) asaphids developed different enrolment styles, giving them a capacity to occupy different ecological niches and a greater range of environments.

Finally, the quantification of the impact of such vital functions on enrolment, as well as on the global cephalon shape has not been assessed here and needs further study. Specifically, the next step should be to explore such evolutionary patterns between closely related taxa: (1) with a 'stable' vs 'variable' number of thoracic segments in order to assess morphological integration from a functional and developmental context in trilobites; and (2) from different ecological frameworks and/or from different ages, in order to compare and test whether the function could influence in the developmental modularity and vice versa, and also to understand the evolutionary mechanism behind the Cambrian and/or Ordovician radiations and compare them with Devonian trilobites.

CONCLUSIONS

Our morphometric study explored the evolutionary pattern between closely related taxa that share a 'stable' number of thoracic segments and ecological framework, to minimize environmental differences and focus on the functional and developmental differences in the diversification of phacopid clades. We conclude that:

1. Evolutionary processes operate in both modular spaces, even though it appears stronger with the cephalon than with the pygidium. These differential divergences among modules are likely a consequence of the more complex selection regime affecting the cephalon (in relation to its numerous functions) compared to the pygidium, and the probable weak trade-offs among these functions.
2. In the integrated space, species share the same pattern of covariation. Nevertheless, differentiation and divergence do also operate along this relative common integration, meaning that evolutionary divergences are partly channelled. This pattern may be the result of weak stabilizing selection acting together with directional selection on the module shapes, implying coordinated evolutionary changes between the two modules and differentiation in a certain direction within the morphological space.
3. However, the integration in *Austerops legrandi* appears partly restructured, namely in the pattern of covariation on the pygidium. Such a difference in the way the two modules interact may indicate that directional selection also acted on the enrolment ability of this species. The involvement of the cephalon in several other functions seems to constrain the response of its features contributing to the enrolment by mainly reorganizing the way the pygidium covaries with the cephalon.

We conclude that important evolutionary trade-offs between enrolment and other vital functions of the cephalon might have been operating during the diversification of trilobites.

Acknowledgements. Our work benefited from the constructive remarks and the language corrections provided by two anonymous reviewers. This paper is a contribution to UMR-CNRS 8198 Evo-Eco-Paleo. The authors thank also the Région Hauts-de-France, and the Ministère de l'Enseignement Supérieur et de la Recherche (CPER Climibio), and the European Fund for Regional Economic Development for their financial support.

DATA ARCHIVING STATEMENT

Data for this study are available in the Dryad Digital Repository: <https://doi.org/10.5061/dryad.mp44794>

Editor. Javier Álvaro

REFERENCES

- ADAMS, D. C. and OTÁROLA-CASTILLO, E. 2013. geomorph: an R package for the collection and analysis of geometric morphometric shape data. *Methods in Ecology & Evolution*, **4**, 393–399.
- ALBERCH, P., GOULD, S. J., OSTER, G. F. and WAKE, D. B. 1979. Size and shape in ontogeny and phylogeny. *Paleobiology*, **5**, 296–317.
- ALBERTI, G. K. B. 1969. *Trilobiten des jüngeren Siluriums sowie des Unter- und Mitteldevons*. I. Schweizerbart Science Publishers, Stuttgart, Germany.
- ARMBRUSTER, W. S. and SCHWAEGERLE, K. E. 1996. Causes of covariation of phenotypic traits among populations. *Journal of Evolutionary Biology*, **9**, 261–276.
- PELABON, C., HANSEN, T. F. and MULDER, C. P. H. 2004. Floral integration and modularity, distinguishing complex adaptations from genetic constraints. 23–49. In PIGLIUCCI, P. and PRESTON, K. A. (eds). *Phenotypic integration: Studying the ecology and evolution of complex phenotypes*. Oxford University Press.
- BOLSTAD, G. H. and HANSEN, T. F. 2014. Integrated phenotypes: understanding trait covariation in plants and animals. *Philosophical Transactions of the Royal Society B*, **369**, 20130245.
- BABCOCK, L. E. and SPEYER, S. E. 1987. Enrolled trilobites from the Alden Pyrite Bed, Ledyard Shale (Middle Devonian) of western New York. *Journal of Paleontology*, **61** (3), 539–548.
- BALLERIO, A. and GREBENNIKOV, V. V. 2016. Rolling into a ball: phylogeny of the Ceratocanthinae (Coleoptera: Hybosoridae) inferred from adult morphology and origin of a unique body enrolment coadaptation in terrestrial arthropods. *Arthropod Systematics & Phylogeny*, **74** (1), 23–52.
- BASSE, M. 2006. *Eifel-Trilobiten IV. Proetida* (3), *Phacopida* (3). Goldschneck, Quelle & Meyer Verlag, Wiebelsheim, 304 pp.
- BENJAMINI, Y. and HOCHBERG, Y. 1995. Controlling the false discovery rate: a practical and powerful approach to multiple testing. *Journal of the Royal Statistical Society Series B (Methodological)*, **57** (1), 289–300.
- BREUKER, C. J., DEBAT, V. and KLINGENBERG, C. P. 2006. Functional evo-devo. *Trends in Ecology & Evolution*, **21**, 488–492.
- BRUTON, D. L. and HAAS, W. 1997. Functional morphology of Phacopinae (Trilobita) and the mechanics of enrolment. *Palaeontographica Abt. A*, **245**, 1–43.
- CAMPBELL, K. S. W. 1977. The functional anatomy of phacopid trilobites: musculature and eyes. *Journal & Proceedings of the Royal Society of New South Wales*, **108**, 168–188.
- CAMPBELL, G. P. and CURRAN, J. M. 2009. The interpretation of elemental composition measurements from forensic glass evidence III. *Science & Justice*, **49**(1), 2–7.
- CARDINI, A. 2016. Lost in the other half: improving accuracy in geometric morphometric analyses of one side of bilaterally symmetric structures. *Systematic Biology*, **65**, 1096–1106.
- CHATTERTON, B., FORTEY, R., BRETT, K., GIBB, S. and McKELLAR, R. 2006. Trilobites from the upper Lower to Middle Devonian Timrhannhart Formation, Jbel Gara el Zguilma, southern Morocco. *Palaeontographica Canadiana*, **25**, 1–177.

- CLARKSON, E. N. K. and HENRY, J. L. 1973. Structure coaptatives et enroulement chez quelques Trilobites ordovi-ciens et siluriens. *Lethaia*, **6** (2), 105–132.
- and WHITTINGTON, H. B. 1997. Enrollment and coaptative structures. 67–74. In KAESLER, R. L. (ed.) *Treatise on invertebrate paleontology. Part O. Arthropoda 1. Trilobita (revised)*. Geological Society of America & University of Kansas Press.
- CLUNE, J., MOURET, J.-B. and LIPSON, H. 2013. The evolutionary origins of modularity. *Proceedings of the Royal Society B*, **280**, 20122863.
- COUETTE, S. and WHITE, J. 2010. 3D geometric morphometrics and missing-data. Can extant taxa give clues for the analysis of fossil primates? *Comptes Rendus Palevol*, **9**, 423–433.
- CRÔNIER, C. and COURVILLE, P. 2003. Variations du rythme du développement chez les trilobites Phacopidae néodévonien. *Comptes Rendus Palevol*, **2**, 577–585.
- BIGNON, A. and FRANÇOIS, A. 2011. Morphological and ontogenetic criteria for defining a trilobite species: the example of Siluro-Devonian Phacopidae. *Comptes Rendus Palevol*, **10**, 143–153.
- DRYDEN, I. L. and MARDIA, K. V. 1998. *Statistical shape analysis*. Wiley Series in Probability and Statistics. Wiley.
- EBLE, G. J. 2005. Morphological modularity and macroevolution: conceptual and empirical aspects. 221–238. In CALLEBAUT, W. and RASSKIN-GUTMAN, D. (eds). *Modularity: Understanding the development and evolution of natural complex systems*. MIT Press, Cambridge MA.
- ELDRIDGE, N. and GOULD, S. J. 1972. Punctuated equilibria: an alternative to phyletic gradualism. 81–115. In SCHOPF, T. J. M. (ed.) *Models in paleobiology*. Freeman, Cooper & Co.
- ESTEVE, J. and YUAN, J. L. 2017. Palaeoecology and evolutionary implications of enrolled trilobites from the Kushan Formation, Guzhangian of North China. *Historical Biology*, **29** (3), 328–340.
- HUGHES, N. C. and ZAMORA, S. 2011. The Purujosa trilobite assemblage and the evolution of trilobite enrollment. *Geology*, **39** (6), 575–578.
- GUTIERREZ-MARCO, J. C., RUBIO, P. and RABANO, I. 2018. Evolution of trilobite enrolment during the Great Ordovician Biodiversification Event: insights from kinematic modelling. *Lethaia*, **51** (2), 207–217.
- FORTEY, R. A. and OWENS, R. M. 1999. Feeding habits in trilobites. *Palaentology*, **42**, 429–465.
- GERBER, S. 2014. Not all roads can be taken: development induces anisotropic accessibility in morphospace. *Evolution & Development*, **16**, 373–381.
- and HOPKINS, M. J. 2011. Mosaic heterochrony and evolutionary modularity: the trilobite genus *Zacanthopsis* as a case study. *Evolution*, **65**, 3241–3252.
- NEIGE, P. and EBLE, G. J. 2007. Combining ontogenetic and evolutionary scales of morphological disparity: a study of early Jurassic ammonites: morphological disparity and developmental dynamics. *Evolution & Development*, **9**, 472–482.
- EBLE, G. J. and NEIGE, P. 2008. Allometric space and allometric disparity: a developmental perspective in the macroevolutionary analysis of morphological disparity. *Evolution*, **62**, 1450–1457.
- GOULD, S. J. 1977. *Ontogeny and phylogeny*. Harvard University Press, Cambridge MA. 503 pp.
- 1998. Heterochrony. 158–165. In FOX KELLER, E. and LLOYD, E. A. (eds). *Keywords in evolutionary biology*. Harvard University Press, Cambridge MA.
- GUILLAUME, F. and OTTO, S. P. 2012. Gene functional trade-offs and the evolution of pleiotropy. *Genetics*, **192**, 1389.
- GUNZ, P., MITTEROECKER, P., NEUBAUER, S., WEBER, G. W. and BOOKSTEIN, F. L. 2009. Principles for the virtual reconstruction of hominin crania. *Journal of Human Evolution*, **57**, 48–62.
- HALLGRÍMSSON, B., JAMNICZKY, H., YOUNG, N. M., ROLIAN, C., PARSONS, T. E., BOUGHNER, J. C. and MARCUCIO, R. S. 2009. Deciphering the palimpsest: studying the relationship between morphological integration and phenotypic covariation. *Evolutionary Biology*, **36**, 355–376.
- HAUG, C. and HAUG, J. 2014. Defensive enrolment in mantis shrimp larvae (Malacostraca: Stomatopoda). *Contributions to Zoology*, **83** (3), 185–194.
- HENRY, J. L. and CLARKSON, E. N. K. 1974. Enrollment and coaptations in some species of the Ordovician trilobite genus *Placoparia*. *Fossils & Strata*, **4**, 87–95.
- HUGHES, N. C. 2003. Trilobite body patterning and the evolution of arthropod tagmosis. *BioEssays*, **25**, 386–395.
- 2007. The evolution of trilobite body patterning. *Annual Review of Earth & Planetary Sciences*, **35**, 401–434.
- MINELLI, A. and FUSCO, G. 2006. The ontogeny of trilobite segmentation: a comparative approach. *Paleobiology*, **32**, 602–627.
- HUPÉ, P. 1953. Classification des trilobites. *Annales de Paléontologie*, **39**, 1–110.
- JABLONSKI, D. 2000. Micro- and macroevolution: scale and hierarchy in evolutionary biology and paleobiology. *Paleobiology*, **26**, 15–52.
- KHALDI, A. Y., CRÔNIER, C., HAINAUT, G., ABBACHE, A. and OUALI MEHADJI, A. 2016. A trilobite faunule from the Lower Devonian of the Saoura Valley, Algeria: biodiversity, morphological variability and palaeobiogeographical affinities. *Geological Magazine*, **153**, 357–387.
- KLINGENBERG, C. P. 2008. Morphological integration and developmental modularity. *Annual Review of Ecology, Evolution, & Systematics*, **39**, 115–132.
- 2014. Studying morphological integration and modularity at multiple levels: concepts and analysis. *Philosophical Transactions of the Royal Society B*, **369**, 20130249.
- and MCINTYRE, G. S. 1998. Geometric morphometrics of developmental instability: analyzing patterns of fluctuating asymmetry with Procrustes methods. *Evolution*, **52**, 1363–1375.
- MEBUS, K. and AUFRAY, J.-C. 2003. Developmental integration in a complex morphological structure: how distinct are the modules in the mouse mandible? *Evolution & Development*, **5**, 522–531.
- KLUG, C., SCHULZ, H. and DE BAETS, K. 2009. Red Devonian trilobites with green eyes from Morocco and the silicification of the trilobite exoskeleton. *Acta Palaeontologica Polonica*, **54**, 117–123.

- LAIBL, L., ESTEVE, J. and FATKA, O. 2016. Enrollment and thoracic morphology in paradoxid trilobites from the Cambrian of the Czech Republic. *Fossil Imprint*, **72** (3–4), 161–171, Praha.
- LE MAÎTRE, D. 1952. La faune du Dévonien inférieur et moyen de la Saoura et des abords de l'Erg el Djemel (Sud oranais). *Mémoire de la Carte géologique de l'Algérie*, **12**, 1–170.
- LEROSEY-AUBRIL, R. and ANGIOLINI, L. 2009. Permian trilobites from Antalya Province, Turkey, and enrollment in Late Palaeozoic Trilobites. *Turkish Journal of Earth Sciences*, **18** (3), 427–448.
- MACHADO, F. A., ZAHN, T. M. G. and MARROIG, G. 2018. Evolution of morphological integration in the skull of Carnivora (Mammalia): changes in Canidae lead to increased evolutionary potential of facial traits. *Evolution*, **72** (7), 1399–1419.
- McKELLAR, R. C. and CHATTERTON, B. D. E. 2009. *Early and Middle Devonian Phacopidae (Trilobita) of southern Morocco. Palaeontographica Canadiana*. Canadian Society of Petroleum Geologists/Geological Association of Canada, St. John's, NF.
- McNAMARA, K. J. 1986. Techniques of exuviation in Australian species of the Cambrian trilobite *Redlichia*. *Alcheringa*, **10**, 403–412.
- MITTEROECKER, P. and BOOKSTEIN, F. 2007. The conceptual and statistical relationship between modularity and morphological integration. *Systematic Biology*, **56**, 818–836.
- . 2008. The evolutionary role of modularity and integration in the hominoid cranium: modularity and integration in the hominoid cranium. *Evolution*, **62**, 943–958.
- ORTEGA-HERNÁNDEZ, J., ESTEVE, J. and BUTTERFIELD, N. J. 2013. Humble origins for a successful strategy: complete enrollment in early Cambrian olenellid trilobites. *Biological Letters*, **9**, 20130679 (5 pp).
- OUDOT, M., CRÔNIER, C., NEIGE, P. and HOLLOWAY, D. 2019a. Phylogeny of some Devonian trilobites based on morphological characters and consequences to the systematics of *Austerops* (Phacopidae). *Journal of Systematic Palaeontology*, **17**, 775–790.
- , NEIGE, P., LAFFONT, R., NAVARRO, N., KHALDI, Y. and CRÔNIER, C. 2019b. Data from: Functional integration for enrolment constrains evolutionary variation of Phacopidae trilobites despite developmental modularity. *Dryad Digital Repository*. <https://doi.org/10.5061/dryad.mp44794>
- PENNA, A., MELO, D., BERNARDI, S., OYARZABAL, M. I. and MARROIG, G. 2017. The evolution of phenotypic integration: how directional selection reshapes covariation in mice. *Evolution*, **71** (10), 2370–2380.
- ROHLF, F. J. 2004. tpsDig: digitize coordinates of landmarks and capture outlines. v. 1.40. Department of Ecology & Evolution, State University of New York at Stony Brook. <http://life.bio.sunysb.edu/morph>
- . 2015. The tps series of software. *Hystrix, the Italian Journal of Mammalogy*, **26**, 9–12.
- and CORTI, M. 2000. Use of two-block partial least-squares to study covariation in shape. *Systematic Biology*, **49**, 740–753.
- ROY, K. and FOOTE, M. 1997. Morphological approaches to measuring biodiversity. *Trends in Ecology & Evolution*, **12** (7), 277–281.
- RUEFFLER, C., HERMISSON, J. and WAGNER, G. P. 2012. Evolution of functional specialization and division of labor. *Proceedings of the National Academy of Sciences*, **109**, E326–E335.
- SPEYER, S. E. 1988. Biostratigraphy and functional morphology of enrollment in two Middle Devonian trilobites. *Lethaia*, **21**, 121–138.
- VIERSEN, A. P. VAN, HOLLAND, D. and KOPPKA, J. 2017. The phacopine trilobite genera *Morocops* Basse, 2006 and *Adrisiops* gen. nov. from the Devonian of Morocco. *Bulletin of Geosciences*, **92**, 13–30.
- WAGNER, G. P. 1996. Homologues, natural kinds and the evolution of modularity. *American Zoologist*, **36**, 36–43.
- and ALTENBERG, L. 1996. Perspective: complex adaptations and the evolution of evolvability. *Evolution*, **50**, 967.
- WHITTINGTON, H. B., CHATTERTON, B. D. E., SPEYER, S. E., FORTEY, R. A., OWENS, R. M., CHANG, W. T., DEAN, W. T., JELL, P. A., LAURIE, J. R., PALMER, A. R., REPINA, L. N., RUSHTON, A. W. A., SHERGOLD, J. H., CLARKSON, E. N. K., WILMONT, N. V. and KELLY, S. R. A. 1997. *Treatise on invertebrate paleontology. Part O. Arthropoda 1. Trilobita (revised)*. Geological Society of America & University of Kansas Press. 530 pp.
- YOUNG, N. M. 2006. Function, ontogeny and canalization of shape variance in the primate scapula. *Journal of Anatomy*, **209** (5), 623–636.